ACS Infectious Diseases

pubs.acs.org/journal/aidcbc

Article

Non-Neutralizing Epitopes Shade Neutralizing Epitopes against Omicron in a Multiple Epitope-Based Vaccine

Hua-Rui Gong,[¶] Ye-fan Hu,[¶] Xuechen Li, Thomas Yau, Bao-Zhong Zhang,* and Jian-Dong Huang*

Cite This: https://doi.org/10.1021/acsinfecdis.2c00488

Read Online

ACCESS | Metrics & More | Article Recommendations

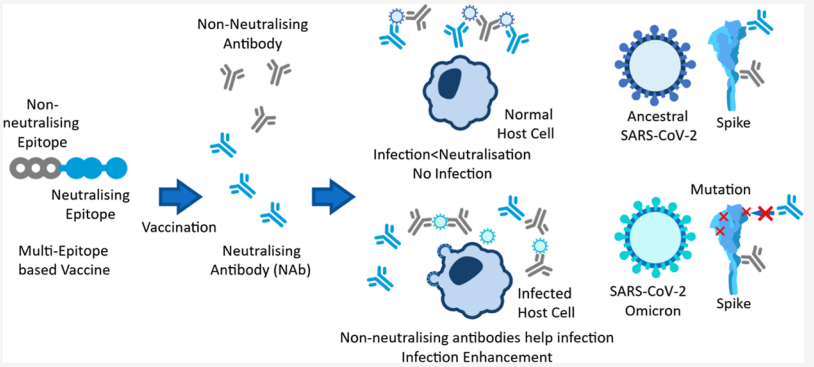

ABSTRACT: The ongoing coronavirus disease 2019 pandemic has raised concerns about the risk of re-infection. Non-neutralizing epitopes are one of the major reasons for antibody-dependent enhancement. Past studies on the ancestral severe acute respiratory syndrome coronavirus 2 (SARS-CoV-2) have revealed an infectivity-enhancing site on the ancestral SARS-CoV-2 spike protein. However, infection enhancement associated with the SARS-CoV-2 Omicron strain remains elusive. In this study, we examined the antibodies induced by a multiple epitope-based vaccine, which showed infection enhancement for the Omicron strain but not for the ancestral SARS-CoV-2 or Delta strain. By examining the antibodies induced by single epitope-based vaccines, we identified a conserved epitope, IDf (450−469), with neutralizing activity against ancestral SARS-CoV-2, Delta, and Omicron. Although neutralizing epitopes are present in the multiple epitope-based vaccine, other immunodominant non-neutralizing epitopes such as IDg (480−499) can shade their neutralizing activity, leading to infection enhancement of Omicron. Our study provides up-to-date epitope information on SARS-CoV-2 variants to help design better vaccines or antibody-based therapeutics against future variants.

KEYWORDS: *SARS-CoV-2, variants, antibody, neutralization, linear epitopes, immunodominant site*

INTRODUCTION

The ongoing coronavirus disease 2019 (COVID-19) pandemic caused by severe acute respiratory syndrome coronavirus 2 (SARS-CoV-2) has resulted in more than 614 million COVID-19 cases worldwide as of September 2022. The increased risk of SARS-CoV-2 re-infection or breakthrough infection has led to repeated waves of infections. A major reason is that neutralizing antibody titers have reduced the neutralizing activity against some variants.[1] Furthermore, the detected humoral responses in terms of the neutralizing antibody titer represent the overall effect of neutralizing and non-neutralizing antibodies. Current studies have mainly focused on immune escape caused by multiple mutations on the spike protein. In addition to immune escape, infectivity-enhancing non-neutralizing epitopes can increase the risk of re-infection.[2] However, non-neutralizing antibodies induced by vaccines have not been well studied. We used linear epitope-based vaccines to show that the overall neutralizing activity of a vaccine is a balance between neutralizing and non-neutralizing antibodies.

Past studies have reported infectivity-enhancing epitopes on the spike protein of the coronavirus, leading to antibody-dependent enhancement (ADE) and acute lung injury.[3] Such enhancement can be noticed due to the immunodominance. Some epitopes elicit stronger antibody-mediated and cell-mediated immunity and are referred to as immunodominant, while other epitopes induce no or weak immunological responses and are referred to as subdominant epitopes.[4] Infection enhancement was shown to be induced by a single SARS-CoV-1 linear immunodominant epitope, LYQDVNC, which is recognized by the monoclonal antibody 43-3-14.[5]

Received: September 27, 2022

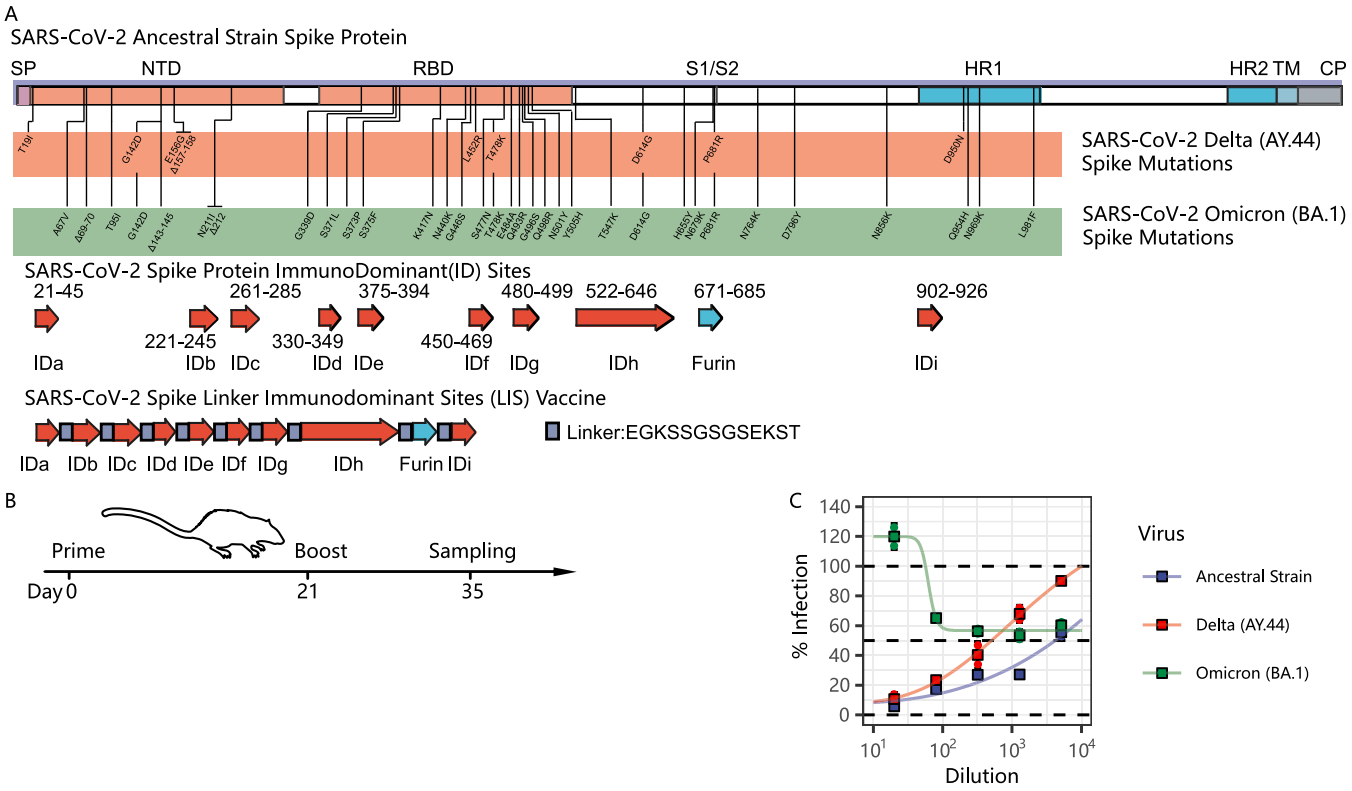

Figure 1. Immune responses induced by a multiple epitope-based vaccine. (A) Construction of the LIS vaccine, a multiple epitope-based vaccine. (B) Immunization and sample processing of the multiple epitope-based LIS vaccine. (C) Neutralizing activity of the LIS vaccine against the ancestral, Delta, and Omicron strains; single linear immunodominant sites and their immune responses.

This infectivity-enhancing epitope is conserved in both SARS-CoV-1 and ancestral SARS-CoV-2. In the ancestral SARS-CoV-2, this fragment is found in 611−617 of the spike protein. However, this epitope changed due to the dominant D614G mutation. More recent studies have revealed for the first time infectivity-enhancing antibodies and pairwise epitopes on the N-terminal domain (NTD) and receptor-binding domain (RBD) of the ancestral SARS-CoV-2 spike protein.[6,7] Moreover, infectivity-enhancing mutations, such as Q498H, have also been reported in a lethal mouse model.[8]

Recently, it was reported in South Africa that the Omicron strain can lead to increased risk of re-infection or breakthrough infection.[9] Considering the association between non-neutralizing antibodies and re-infection, the non-neutralizing antibodies induced by vaccines based on the ancestral spike protein should be further tested against Omicron. However, it may be challenging to investigate the balance between neutralizing and non-neutralizing antibodies against Omicron because the Omicron spike protein has multiple critical mutations. The antigenicity of most conformational epitopes can be shifted by only one or two mutations. For example, two alterations, K417N and E484K, led to antigenic drift in the Beta and Gamma variants.[10] As the Omicron spike has over 30 mutations, it is important to use an optimized model for further study.

To study the balance of neutralizing and non-neutralizing antibodies, a linear epitope-based vaccine would be a better model than a conformational epitope-based vaccine. Previous studies showed that linear epitopes are conserved across multiple coronaviruses with cross-reactivity.[11] Moreover, a multiple linear epitope-based vaccine has been developed that shows effectiveness in an animal model.[12] In a multiple linear epitope-based vaccine, if one epitope is destroyed by a single mutation, the other linear epitopes might be less impacted. At the same time, we need to detect how mutations impact each epitope separately. A single epitope-based vaccine can be easily generated using the hepatitis B core (HBc) protein virus-like particle (VLP)-based[13] SpyCatcher/SpyTag system.[14] In this way, both multiple epitope-based and single epitope-based vaccines can be utilized to show the integrated and separate effects of neutralizing and non-neutralizing antibodies induced by linear epitopes.

In this study, we examined the effects of neutralizing and non-neutralizing antibodies induced by a multiple linear epitope-based vaccine against multiple variants including ancestral SARS-CoV-2, Delta, and Omicron strains. We further studied the combined and individual effects of neutralizing and non-neutralizing antibodies induced by single linear epitope-based vaccines. These findings can provide up-to-date epitope information on SARS-CoV-2 variants to help design vaccines or antibody-based therapeutics against future variants.

RESULTS

Multiple Epitope-Based LIS Vaccine against SARS-CoV-2 Variants. We examine the linker-immunodominant site (LIS) vaccine, a multiple epitope-based vaccine, against multiple variants including ancestral SARS-CoV-2, Delta (AY.44), and Omicron (B.1.15) (Figure 1A). This LIS vaccine can induce epitope-specific immunoglobulin (IgG) and offers effective protection in animals challenged with the live virus.[12] This vaccine contains 10 fragments (IDa-IDi plus Furin) linked by linkers (Figure 1A). The nine linear immunodominant sites (IDa-IDi) on the spike protein were first identified in convalescent sera from COVID-19 patients.[15] Three sites are

https://doi.org/10.1021/acsinfecdis.2c00488
ACS Infect. Dis. XXXX, XXX, XXX−XXX

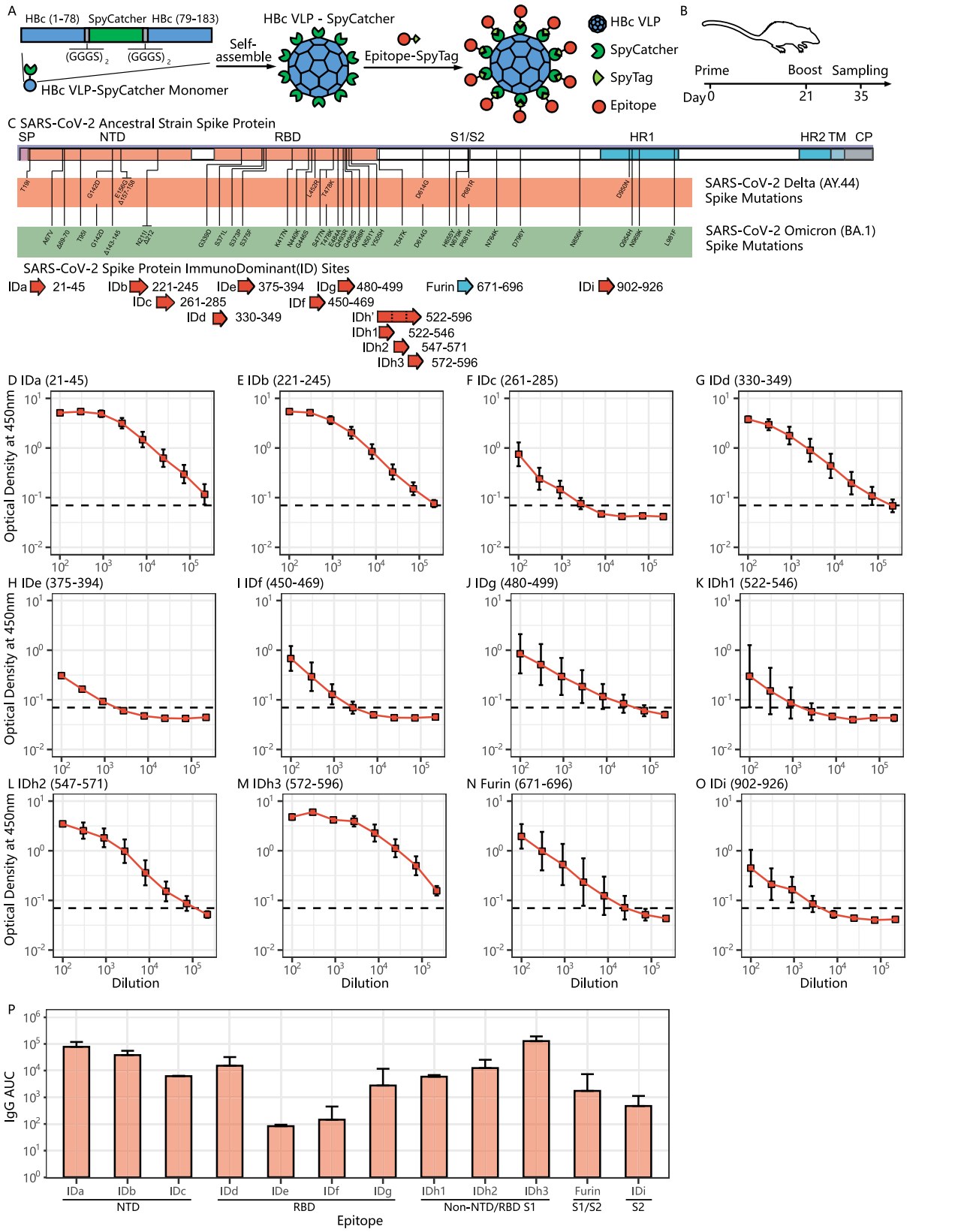

Figure 2. Immune responses induced by single epitope-based vaccines. (A) Construction of single epitope-based vaccines using HBV core protein VLPs and the SpyCatcher/SpyTag system. (B) Immunization and sample processing of single epitope-based vaccines. (C) Spike protein and immunodominant sites. (D−O) Optical density at 450 nm of epitope-specific IgG induced by IDa, IDb, IDc, IDd, IDe, IDf, IDg, IDh1, IDh2, IDh3, furin, and IDi. The dashed line shows the cut-off value of the optical density (0.07) for the AUC calculation. (P) AUC of epitope-specific IgG; neutralization activities of a single linear epitope against SARS-CoV-2 variants.

https://doi.org/10.1021/acsinfecdis.2c00488
ACS Infect. Dis. XXXX, XXX, XXX−XXX

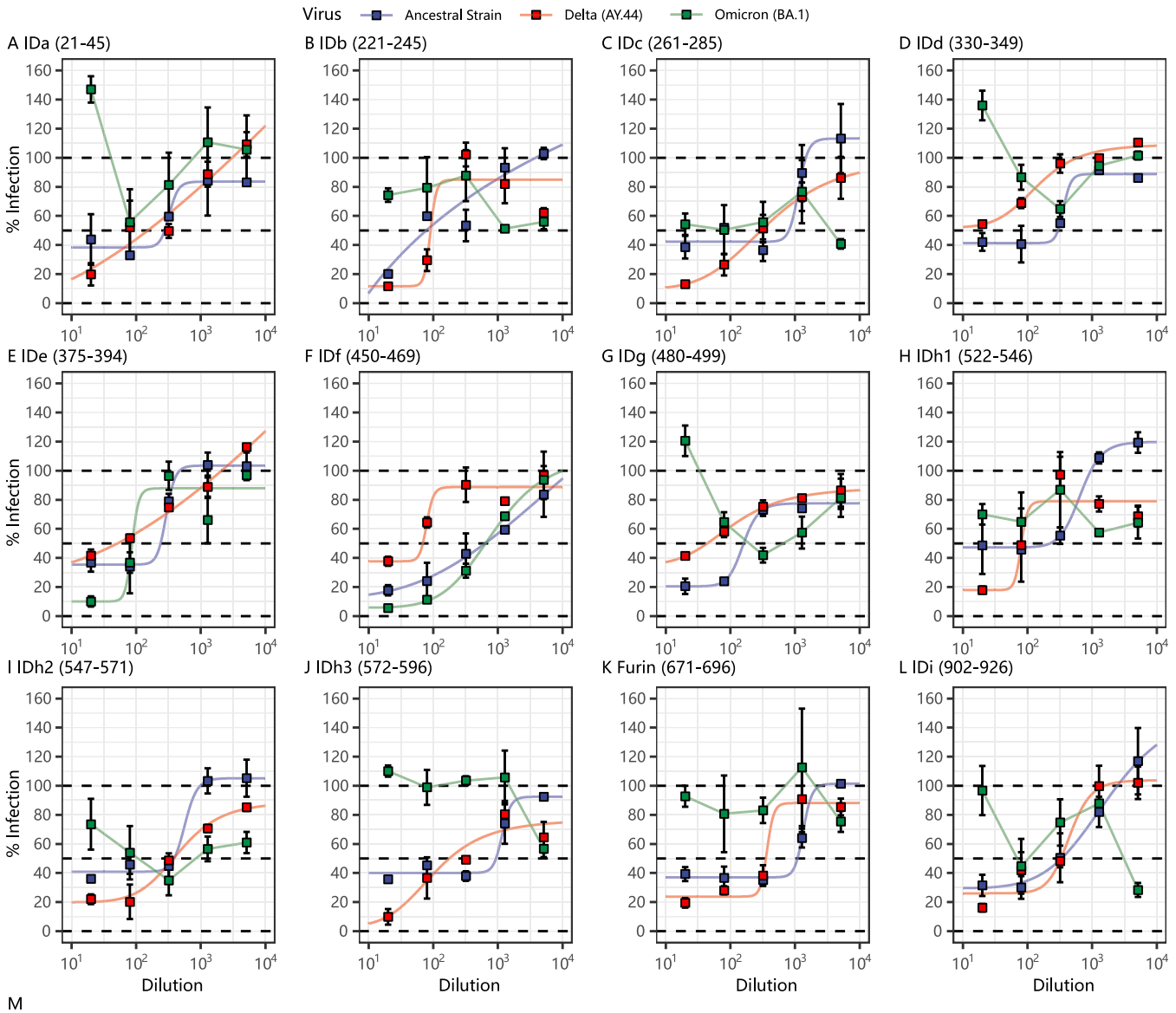

M

	IDa	IDb	IDc	IDd	IDe	IDf	IDg	IDh1	IDh2	IDh3	Furin	IDi	LIS
The Ancestral Stain	266.9	77.551	897.83	299.74	220.87	633.84	160.74	218.89	386.51	981.52	1091.7	335.7	4108.36
Delta (AY.44)	152.73	92.04	306.44	<20	50.67	62.34	42.22	80.61	391.35	183.92	356.74	309.85	509.89
Omicron (BA.1)	NA	NA	NA	NA	85.841	645.33	NA	NA	NA	NA	NA	NA	NA

Figure 3. Neutralizing activity of single epitope-based vaccines against the ancestral, Delta, and Omicron strains. The neutralization curves of (A) IDa, (B) IDb, (C) IDc, (D) IDd, (E) IDe, (F) IDf, (G) IDg, (H) IDh1, (I) IDh2, (J) IDh3, (K) furin, and (L) IDi. (M) 50% inhibitory dose (ID_{50}) of each vaccine against the ancestral, Delta, and Omicron strains.

in the NTD, four are in the RBD, and one site, IDh, is located in the non-NTD/RBD S1 fragment. After primer and booster vaccinations, blood samples were collected from mice to measure the neutralizing activity (Figure 1B). The LIS vaccine showed strong protective immune responses in terms of the pseudotyped virus-based neutralizing antibody titer against ancestral SARS-CoV-2 and Delta, but not Omicron. The LIS vaccine had a 50% inhibitory dose (ID_{50}) or 50% neutralization titer of over 4000 against the ancestral SARS-CoV-2 and about 500 against the Delta strain (Figure 1C). However, the LIS vaccine did not reach 50% inhibition against the Omicron strain (Figure 1C), which means that the neutralizing antibody titer was lower than the cut-off value of 1:20. This significant decrease in the neutralizing antibody titer is not surprising because the mutations on the Delta spike impact only three fragments of LIS (IDf, IDh, and Furin), whereas the mutations on the Omicron spike impact five of the ten fragments (IDd, IDe, IDg, IDh, and Furin). The neutralizing activity of LIS is weakened by the antigenicity changes in the Omicron spike, and even worse, this vaccine induces infection enhancement in Omicron. When the serum samples were diluted to 1:20, we detected a significant increase in the percentage infection. This infection enhancement was similar to the previously reported ADE in human sera.[16] As the neutralizing activity of a multiple epitope-based vaccine is the sum of the immune responses of each epitope, it is necessary to determine whether any of the epitope-specific antibodies are impacted impartially or whether each epitope has a unique response against different variants.

https://doi.org/10.1021/acsinfecdis.2c00488
ACS Infect. Dis. XXXX, XXX, XXX−XXX

To detect the immune responses of individual epitopes, we constructed HBc protein VLPs for each linear immunodominant site using the SpyCatcher/SpyTag system (Figure 2A,B). The HBc VLP-SpyCatcher was constructed by inserting SpyCatcher in between the 78th and 79th residues of HBc with $(GGGS)_2$ linkers on each side. The HBc VLP-SpyCatcher monomers self-assemble into a polymer with 120 copies, which are able to display up to 120 linear epitopes per VLP. To achieve better VLP delivery efficiency, we split the IDh linear immunodominant site into three subsites, IDh1, IDh2, and IDh3 (Figure 2C). All linear epitopes were chemically synthesized by conjugating SpyTag (AHIVMVDAYKPTK) to the N-terminal. After incubating the linear epitope-containing SpyTag with HBc VLP-SpyCatcher at a molar ratio of 3:1 (peptide/VLP), each epitope peptide was rapidly connected to the HBc-VLP to build the single epitope-based vaccines (Figure 2A).

The BALB/c mice were immunized with the HBc-VLPs linked to each linear epitope. After primer and booster vaccinations, we collected serum samples to measure epitope-specific IgG (Figure 2B). Distinct epitopes with different antigenicities induced distinct immune responses, with the linear epitope-specific IgG enzyme-linked immunosorbent assay (ELISA) area under curve (AUC) varying from 10^2 to 10^5 (Figure 2D−O). Some linear epitopes, including IDa, IDb, IDd, IDh2, and IDh3, induced high-specific IgG with ELISA AUC over 10^4 (Figure 2P). Single epitope-based vaccines can induce epitope-specific antibodies that can be further utilized to display the balance of neutralizing and non-neutralizing antibodies.

To illustrate the infection enhancement of Omicron, we performed pseudotyped virus-based neutralization assays using a single epitope to induce polyclonal sera against the ancestral SARS-CoV-2, Delta, and Omicron (Figure 3A−L). We found that all epitopes could induce sufficient neutralizing antibodies to achieve an ID_{50} against the ancestral SARS-CoV-2 (Figure 3). One epitope (Figure 3D) was unable to achieve 50% inhibition against Delta. Comparing the results of the ancestral SARS-CoV-2 and Delta strain, there was an eight-fold decrease in the induced neutralizing antibody titer for each epitope in the LIS vaccine, with the 50% inhibitory dose (ID_{50}) against Delta lower in 10 out of 12 epitopes compared to the ancestral SARS-CoV-2 (Figure 3M). The neutralizing activity results for Omicron were much worse. Over 100% infection was detected at 1:20 dilution for epitopes IDa, IDd, and IDg. These neutralizing curves for the Omicron strain were *V*-shaped curves rather than the standard *S*-shaped curves (Figure 3A,D,G). Out of the 12 epitopes, only two epitopes showed 50% inhibition against Omicron (Figure 3E,F). The IDe and IDf epitopes showed standard S-shaped neutralizing curves with a 50% inhibitory dose (ID_{50}) of 85.841 and 645.33, respectively (Figure 3E,F,M). The titer of IDe (375−394)-specific antibodies against Omicron was dampened due to one mutation at the N-terminal of IDe (S375F), whereas IDf (450−469)-specific antibodies showed the highest resistance to Omicron as there were no mutations in IDf.

The LIS-induced infection enhancement of Omicron can be explained using the results from single epitope-based vaccines against Omicron. The results suggest that non-neutralizing epitopes shade neutralizing epitopes against Omicron in the multiple epitope-based LIS vaccine (Figure 1C) even with two epitopes with neutralizing activity against Omicron (Figure 3E,F).

DISCUSSION

In this study, we compared the neutralizing activities of single epitope-based vaccines and a multiple epitope-based LIS vaccine against ancestral SARS-CoV-2, Delta, and Omicron strains. Our results identified a conserved epitope IDf (450−469) with cross-neutralizing activity and some infectivity-enhancing epitopes.

By investigating the single epitope-based vaccines, we found that the balance of neutralizing and non-neutralizing antibodies in the multiple epitope-based vaccine might affect the overall neutralizing activity of the vaccine. We found several epitopes that can induce infection enhancement (Figure 1C) in Omicron. We identified that sites IDa, IDd, and IDg showed infection enhancement at a 1:20 dilution with *V*-shaped neutralizing curves, whereas most sites showed no neutralizing activity against Omicron (Figure 3). Two sites, IDe and IDf, showed neutralizing activity against Omicron when the single epitope-based vaccines were analyzed (Figure 3E,F). Their neutralization activities were masked by other non-neutralizing epitopes in the multiple epitope-based LIS vaccine.

The masking of the neutralizing activity might be a result of immunodominance as our results suggest that immunodominant non-neutralizing epitopes in the vaccine can shade other neutralizing epitopes. The multiple epitope-based LIS vaccine has three immunodominant epitopes, IDg, IDh, and Furin.[12] One immunodominant epitope IDg (480−499) showed infection enhancement. This epitope is similar to previously reported SARS-CoV-2 spike immunodominant sites[17] and infectivity-enhancing epitopes.[7] This fragment shares most of the residues of a conformational immunodominant site (G446, Y449, N481, G482, V483, E484, G485, F486, F490, and S494), which is recognized by a monoclonal antibody S2H13. This epitope is immunodominant in the population, with 100% seropositivity in hospitalized patients, 57% seropositivity in symptomatic patients, and 74% seropositivity in non-symptomatic patients.[17] The immunodominant linear epitope IDg (480−499) was shown to have 51.2% seropositivity in convalescent patients.[15] This fragment also shares most of the residues of an infectivity-enhancing epitope, RBD cluster 1 (Y449, L452, T470, N481, G482, V483, E484, G485, F486, F490, L492, Q493, and S494).[7] This suggests that this highly immunogenic epitope can induce more antibodies compared to other epitopes in the vaccine, and these antibodies are more likely to be infectivity-enhancing antibodies.

Our findings might help the future ADE studies in SARS-CoV-2. ADE is an antibody-mediated increase of viral entrance into immune cells with Fc receptors[18] or other cells without Fc receptors.[6,7] This effect has been observed in flavivirus infections spread by mosquitoes, including Dengue[19] and Zika viruses.[20] For coronaviruses, ADE has mostly been observed in animal models infected with SARS-CoV, MERS-CoV, and feline coronaviruses, where it was found that vaccination-protected animals developed worsened lung illness after infection with the viruses.[3,21,22]

It is crucial to note that the prozone effect may have nothing to do with the above infection enhancement. Hook effect usually occurs because of antigen excess. Some previous studies also reported similar phenomena (prozone effect) due to antibody excess in the agglutination test.[23] This is because excessive antibodies might bind to all the antigens and block all the epitope sites, while limited antibodies are able to bind more than one antigenic particle (pathogen) simultaneously

https://doi.org/10.1021/acsinfecdis.2c00488
ACS Infect. Dis. XXXX, XXX, XXX−XXX

and cause cross-linking. Thus, no subsequent agglutination reaction occurs in the excess of antibodies. The neutralization test is different from the agglutination test. In the neutralization test, viruses are overdosed. If antibodies can bind to viruses, the infection will be inhibited. Even if excessive antibodies inhibit the antibody−antigen cross-linking, it will not lead to a higher infection level than that with low or no neutralizing antibodies. It is difficult to use the prozone effect to explain why more viruses can infect host cells (infection >100%). One possible explanation for the >100% infection is that some non-neutralizing antibodies enhance the viral infectivity, thus increasing the infection percentage over 100%.

We identified a relatively conserved epitope IDf (450−469), which is consistent with RBD E6 (454−463) and E7 (459−471) identified in a previous study.[11] The IDf (450−469) epitope showed high cross-reactivity against SARS-CoV-1 and SARS-CoV-2[11] and cross-neutralizing activity against the ancestral SARS-CoV-2, Delta, and Omicron (Figure 3F). This epitope has also been used in other epitope-based vaccines, which showed humoral immune responses against Alpha, Beta, and Delta.[24] Therefore, the highly conserved IDf (450−469) epitope should be utilized to develop the next-generation pan-coronavirus vaccine rather than the infectivity-enhancing IDg (480−499) epitope. In the research on antibody escape, it was reported that the fragment IDf (450−469) contains two escape sites with higher escape possibility, L455 and F456.[25] This might weaken mutation resistance of linear epitope RBD E6 (454−463) rather than RBD E7 (459−471). In this way, a well-designed linear epitope-based vaccine containing RBD E7 (459−471) might help to generate a pan-coronavirus vaccine.

Overall, we observed that the multiple epitope-based LIS vaccine induced infection enhancement for the Omicron variant. Using single epitope-based vaccines, we discovered that the conserved epitope IDf (450−469) exhibited a neutralizing effect against ancestral SARS-CoV-2, Delta, and Omicron, whereas IDg (480−499) was an infectivity-enhancing epitope for Omicron. This suggests that immunodominant non-neutralizing epitopes might shade neutralizing epitopes in the multiple epitope-based vaccine, leading to infection enhancement in Omicron. This study provides up-to-date epitope information of SARS-CoV-2 variants to help design vaccines or antibody-based therapeutics against future variants.

METHODS

Cell Culture. The human embryonic kidney 293T cell line was obtained from ATCC. Cells were maintained at all times in Dulbecco's modified Eagle's medium supplemented with 10% fetal bovine serum and 1% penicillin−streptomycin. All cells were cultured in a humidified incubator in 5% CO_2 at 37 °C.

Synthesis of Peptides. All SpyTag (AHIVMVDAYKPTK)-conjugated peptides were synthesized by GL Biochem (Shanghai) Ltd. as dry powders. The peptides were generated using solid phase synthesis techniques, and the quality of the final product was analyzed by mass spectrometry. All peptides were dissolved in either pH 7.4 phosphate-buffered saline (PBS) buffer or 4 M pH 7.0 urea Na_2HPO_4/NaH_2PO_4 buffer.

Expression and Purification of HBc VLP-SpyCatcher. The SpyCatcher gene was engineered into a pET28a-HBV core protein-based VLP (VLP-SpyCatcher) in our laboratory. The VLP-SpyCatcher was then expressed in *E. coli* BL21(DE3) RIPL cells. A single colony was selected from the cells cultured on the LB agar plate. The colony was cultured in LB broth (100 μg/mL Ampicillin) at 37 °C with shaking at 220 rpm for 16 h. The preculture was diluted by 1:100 in 1 L of LB broth (100 μg/mL Ampicillin) and then further cultured at 37 °C with shaking at 220 rpm until an OD600 of 0.8 was achieved. Next, 0.5 M isopropyl β-D-1-thiogalactopyranoside was added to the LB broth at a 1:1000 dilution to induce protein expression and further incubated at 32 °C with shaking at 220 rpm for 6 h. After centrifugation, the cell pellet was collected and resuspended in PBS, followed by sonication on ice for 30 min. The bacterial debris was removed by centrifugation at 16,000*g* at 4 °C for 1 h. The supernatant was collected and filtered through a 0.22 μm syringe filter. The HBc VLP-SpyCatcher was purified by density gradient centrifugation and anion-exchange chromatography. A centrifugal filter unit with 100 kDa cut-off was used to concentrate the purified VLP-SpyCatcher. The concentration of the VLP-SpyCatcher was determined using the bicinchoninic acid test before storing at −80 °C until further use.

Animals. Female 6- to 8-week-old BALB/c mice were supplied by the Laboratory Animal Unit of the University of Hong Kong. The mice were maintained under a 12 h light/dark cycle at ∼23 °C and 40% relative humidity. Each peptide (25 μg) was mixed with VLP-SpyCatcher at a molar ratio of 3:1 (peptides/VLP) and incubated overnight at 4 °C. LIS vaccines (25 μg) were made with an aluminum hydroxide gel adjuvant (alum; 1 mg/mL) at a mass ratio of 1:10. Female BALB/c mice were subcutaneously injected with the HBc VLP-SpyCatcher/SpyTag mixture or LIS−alum mixture (3−5 per group, 25 μg/animal/injection). The mice in the control group were administered an equal dose of HBc VLP-SpyCatcher/SpyTag or alum mixed with PBS. The prime vaccination was administrated on day 0, and a boost vaccination was given on day 21. Blood was collected on day 35 through the tail vein, and serum was isolated and stored at −80 °C until further use. All animal protocols were approved by the Committee on the Use of Live Animals in Teaching and Research of the University of Hong Kong.

Enzyme-Linked Immunosorbent Assay. Serum IgG levels were measured using ELISA as previously described.[15] In brief, 96-well plates (Nunc, Roskilde, Denmark) were coated with peptides overnight at 4 °C at a concentration of 0.5 μg/mL (50 μL/well). After removal of the coating buffer, plates were washed four times in PBS (pH 7.4) containing 0.05% Tween 20 (TBST, Sigma) and then blocked with TBS-5% (w/v) non-fat milk at 37 °C for 3 h. Mice sera were diluted in the blocking buffer and added into the wells and incubated at 37 °C for 1 h. After washing the plates six times in TBST, secondary horseradish peroxidase-conjugated goat anti-mouse IgG antibody (ThermoFisher, Catalogue # 31410) diluted in blocking buffer was added and incubated at 37 °C for 1 h. After washing the plates four times, 3,3′,5,5′-tetramethylbenzidine (Sigma) was added and the reaction was subsequently stopped using 2 M H_2SO_4. Optical density at 450 nm was measured using a Thermo Scientific Varioskan Flash 3001 plate reader.

SARS-CoV-2 Pseudovirus Neutralization Assay. Pseudovirions were produced by co-transfecting 293T cells with psPAX2, pLenti-luciferase, and plasmids encoding the ancestral SARS-CoV-2 spike protein, Delta spike (AY.44, reference sequence: EPI_ISL_7260588), or Omicron spike (BA.1.15,

https://doi.org/10.1021/acsinfecdis.2c00488
ACS Infect. Dis. XXXX, XXX, XXX−XXX

reference sequence: EPI_ISL_8358538) using polyetherimide. The supernatants at 40 and 64 h post-transfection were collected and centrifuged at 2000 rpm for 10 min and then passed through a 0.45 μm filter to remove cell debris and stored at −80 °C until further use. For the neutralization assays, mice sera were heated to 56 °C for 30 min to inactivate the complement. The SARS-CoV-2, Delta, and Omicron pseudovirions were pre-incubated with four-fold serially diluted mice sera, ranging from 1: 20 to 1:5120 for 1 h on ice. The virus−sera mixture was then added onto 293/hACE2 cells in a 96-well plate. After 6 h of incubation, the inoculum was replaced with fresh complete DMEM. Cells were lysed after 40 h by adding 50 μL of steady-Glo reagent (Promega) to each well with an equal volume of culture medium and incubated for 5 min to allow sufficient cell lysis. The luminescence was measured using a Thermo Scientific Varioskan Flash 3001 plate reader.

AUTHOR INFORMATION

Corresponding Authors

Bao-Zhong Zhang − *Chinese Academy of Sciences (CAS) Key Laboratory of Quantitative Engineering Biology, Shenzhen Institute of Synthetic Biology, Shenzhen Institutes of Advanced Technology, Chinese Academy of Sciences, Shenzhen 518055, China*; Email: bz.zhang3@siat.ac.cn

Jian-Dong Huang − *School of Biomedical Sciences, Li Ka Shing Faculty of Medicine, University of Hong Kong, Hong kong 999077, China; Chinese Academy of Sciences (CAS) Key Laboratory of Quantitative Engineering Biology, Shenzhen Institute of Synthetic Biology, Shenzhen Institutes of Advanced Technology, Chinese Academy of Sciences, Shenzhen 518055, China; Department of Clinical Oncology, Shenzhen Key Laboratory for Cancer Metastasis and Personalized Therapy, The University of Hong Kong-Shenzhen Hospital, Shenzhen 518055, China; Guangdong-Hong Kong Joint Laboratory for RNA Medicine, Sun Yat-Sen University, Guangzhou 510120, China*; orcid.org/0000-0002-3798-9874; Email: jdhuang@hku.hk

Authors

Hua-Rui Gong − *School of Biomedical Sciences, Li Ka Shing Faculty of Medicine, University of Hong Kong, Hong kong 999077, China*

Ye-fan Hu − *School of Biomedical Sciences, Li Ka Shing Faculty of Medicine, University of Hong Kong, Hong kong 999077, China; Department of Medicine, School of Clinical Medicine, University of Hong Kong, Hong Kong 999077, China*

Xuechen Li − *Department of Chemistry, University of Hong Kong, Hong Kong 999077, China*; orcid.org/0000-0001-5465-7727

Thomas Yau − *Department of Medicine, School of Clinical Medicine, University of Hong Kong, Hong Kong 999077, China*

Complete contact information is available at: https://pubs.acs.org/10.1021/acsinfecdis.2c00488

Author Contributions

¶H.-R.G. and Y.-f.H. made equal contributions.

Notes

The authors declare no competing financial interest.

ACKNOWLEDGMENTS

The research was supported by the National Key Research and Development Program of China (2021YFA0910700, 2018YFA0902701), the Health and Medical Research Fund, the Food and Health Bureau, the Government of the Hong Kong Special Administrative Region (COVID190117, COVID1903010, T-11-709/21-N) and Guangdong Science and Technology Department (2020B1212030004) to J.H. J.H. thanks the L & T Charitable Foundation, the Program for Guangdong Introducing Innovative and Entrepreneurial Teams (2019BT02Y198), and Shenzhen Key Laboratory for Cancer Metastasis and Personalized Therapy (ZDSYS20210623091811035) for their support.

REFERENCES

(1) Harvey, W. T.; Carabelli, A. M.; Jackson, B.; Gupta, R. K.; Thomson, E. C.; Harrison, E. M.; Ludden, C.; Reeve, R.; Rambaut, A.; Peacock, S. J.; Robertson, D. L.; Consortium, C.-G. U. SARS-CoV-2 variants, spike mutations and immune escape. *Nat. Rev. Microbiol.* **2021**, *19*, 409−424.

(2) Maemura, T.; Kuroda, M.; Armbrust, T.; Yamayoshi, S.; Halfmann, P. J.; Kawaoka, Y.; Schultz-Cherry, S. Antibody-Dependent Enhancement of SARS-CoV-2 Infection Is Mediated by the IgG Receptors FcγRIIA and FcγRIIIA but Does Not Contribute to Aberrant Cytokine Production by Macrophages. *mBio* **2021**, *12*, No. e01987.

(3) Liu, L.; Wei, Q.; Lin, Q.; Fang, J.; Wang, H.; Kwok, H.; Tang, H.; Nishiura, K.; Peng, J.; Tan, Z.; Wu, T.; Cheung, K.-W.; Chan, K.-H.; Alvarez, X.; Qin, C.; Lackner, A.; Perlman, S.; Yuen, K.-Y.; Chen, Z. Anti−spike IgG causes severe acute lung injury by skewing macrophage responses during acute SARS-CoV infection. *JCI Insight* **2019**, *4*, No. e123158.

(4) Akram, A.; Inman, R. D. Immunodominance: A pivotal principle in host response to viral infections. *Clin. Immunol.* **2012**, *143*, 99−115.

(5) Wang, Q.; Zhang, L.; Kuwahara, K.; Li, L.; Liu, Z.; Li, T.; Zhu, H.; Liu, J.; Xu, Y.; Xie, J.; Morioka, H.; Sakaguchi, N.; Qin, C.; Liu, G. Immunodominant SARS Coronavirus Epitopes in Humans Elicited both Enhancing and Neutralizing Effects on Infection in Non-human Primates. *ACS Infect. Dis.* **2016**, *2*, 361−376.

(6) Liu, Y.; Soh, W. T.; Kishikawa, J.-i.; Hirose, M.; Nakayama, E. E.; Li, S.; Sasai, M.; Suzuki, T.; Tada, A.; Arakawa, A.; Matsuoka, S.; Akamatsu, K.; Matsuda, M.; Ono, C.; Torii, S.; Kishida, K.; Jin, H.; Nakai, W.; Arase, N.; Nakagawa, A.; Matsumoto, M.; Nakazaki, Y.; Shindo, Y.; Kohyama, M.; Tomii, K.; Ohmura, K.; Ohshima, S.; Okamoto, T.; Yamamoto, M.; Nakagami, H.; Matsuura, Y.; Nakagawa, A.; Kato, T.; Okada, M.; Standley, D. M.; Shioda, T.; Arase, H. An infectivity-enhancing site on the SARS-CoV-2 spike protein targeted by antibodies. *Cell* **2021**, *184*, 3452−3466.

(7) Li, D.; Edwards, R. J.; Manne, K.; Martinez, D. R.; Schäfer, A.; Alam, S. M.; Wiehe, K.; Lu, X.; Parks, R.; Sutherland, L. L.; Oguin, T. H., III; McDanal, C.; Perez, L. G.; Mansouri, K.; Gobeil, S. M. C.; Janowska, K.; Stalls, V.; Kopp, M.; Cai, F.; Lee, E.; Foulger, A.; Hernandez, G. E.; Sanzone, A.; Tilahun, K.; Jiang, C.; Tse, L. V.; Bock, K. W.; Minai, M.; Nagata, B. M.; Cronin, K.; Gee-Lai, V.; Deyton, M.; Barr, M.; Von Holle, T.; Macintyre, A. N.; Stover, E.; Feldman, J.; Hauser, B. M.; Caradonna, T. M.; Scobey, T. D.; Rountree, W.; Wang, Y.; Moody, M. A.; Cain, D. W.; DeMarco, C. T.; Denny, T. N.; Woods, C. W.; Petzold, E. W.; Schmidt, A. G.; Teng, I. T.; Zhou, T.; Kwong, P. D.; Mascola, J. R.; Graham, B. S.; Moore, I. N.; Seder, R.; Andersen, H.; Lewis, M. G.; Montefiori, D. C.; Sempowski, G. D.; Baric, R. S.; Acharya, P.; Haynes, B. F.; Saunders, K. O. In vitro and in vivo functions of SARS-CoV-2 infection-enhancing and neutralizing antibodies. *Cell* **2021**, *184*, 4203−4219.

(8) Iwata-Yoshikawa, N.; Shiwa, N.; Sekizuka, T.; Sano, K.; Ainai, A.; Hemmi, T.; Kataoka, M.; Kuroda, M.; Hasegawa, H.; Suzuki, T.; Nagata, N. A lethal mouse model for evaluating vaccine-associated

enhanced respiratory disease during SARS-CoV-2 infection. *Sci. Adv.* **2022**, *8*, No. eabh3827.
(9) Pulliam, J. R. C.; van Schalkwyk, C.; Govender, N.; von Gottberg, A.; Cohen, C.; Groome, M. J.; Dushoff, J.; Mlisana, K.; Moultrie, H. Increased risk of SARS-CoV-2 reinfection associated with emergence of Omicron in South Africa. *Science* **2022**, *376*, No. eabn4947.
(10) Yuan, M.; Huang, D.; Lee, C.-C. D.; Wu, N. C.; Jackson, A. M.; Zhu, X.; Liu, H.; Peng, L.; van Gils, M. J.; Sanders, R. W.; Burton, D. R.; Reincke, S. M.; Prüss, H.; Kreye, J.; Nemazee, D.; Ward, A. B.; Wilson, I. A. Structural and functional ramifications of antigenic drift in recent SARS-CoV-2 variants. *Science* **2021**, *373*, 818−823.
(11) Shrock, E.; Fujimura, E.; Kula, T.; Timms, R. T.; Lee, I-H.; Leng, Y.; Robinson, M. L.; Sie, B. M.; Li, M. Z.; Chen, Y.; Logue, J.; Zuiani, A.; McCulloch, D.; Lelis, F. J. N.; Henson, S.; Monaco, D. R.; Travers, M.; Habibi, S.; Clarke, W. A.; Caturegli, P.; Laeyendecker, O.; Piechocka-Trocha, A.; Li, J. Z.; Khatri, A.; Chu, H. Y.; Villani, A.-C.; Kays, K.; Goldberg, M. B.; Hacohen, N.; Filbin, M. R.; Yu, X. G.; Walker, B. D.; Wesemann, D. R.; Larman, H. B.; Lederer, J. A.; Elledge, S. J.; Lavin-Parsons, K.; Parry, B.; Lilley, B.; Lodenstein, C.; McKaig, B.; Charland, N.; Khanna, H.; Margolin, J.; Gonye, A.; Gushterova, I.; Lasalle, T.; Sharma, N.; Russo, B. C.; Rojas-Lopez, M.; Sade-Feldman, M.; Manakongtreecheep, K.; Tantivit, J.; Thomas, M. F.; Abayneh, B. A.; Allen, P.; Antille, D.; Armstrong, K.; Boyce, S.; Braley, J.; Branch, K.; Broderick, K.; Carney, J.; Chan, A.; Davidson, S.; Dougan, M.; Drew, D.; Elliman, A.; Flaherty, K.; Flannery, J.; Forde, P.; Gettings, E.; Griffin, A.; Grimmel, S.; Grinke, K.; Hall, K.; Healy, M.; Henault, D.; Holland, G.; Kayitesi, C.; LaValle, V.; Lu, Y.; Luthern, S.; Marchewka, J.; Martino, B.; McNamara, R.; Nambu, C.; Nelson, S.; Noone, M.; Ommerborn, C.; Pacheco, L. C.; Phan, N.; Porto, F. A.; Ryan, E.; Selleck, K.; Slaughenhaupt, S.; Sheppard, K. S.; Suschana, E.; Wilson, V.; Alter, G.; Balazs, A.; Bals, J.; Barbash, M.; Bartsch, Y.; Boucau, J.; Chevalier, J.; Chowdhury, F.; Einkauf, K.; Fallon, J.; Fedirko, L.; Finn, K.; Garcia-Broncano, P.; Hartana, C.; Jiang, C.; Kaplonek, P.; Karpell, M.; Lam, E. C.; Lefteri, K.; Lian, X.; Lichterfeld, M.; Lingwood, D.; Liu, H.; Liu, J.; Ly, N.; Michell, A.; Millstrom, I.; Miranda, N.; O'Callaghan, C.; Osborn, M.; Pillai, S.; Rassadkina, Y.; Reissis, A.; Ruzicka, F.; Seiger, K.; Sessa, L.; Sharr, C.; Shin, S.; Singh, N.; Sun, W.; Sun, X.; Ticheli, H.; Trocha-Piechocka, A.; Worrall, D.; Zhu, A.; Daley, G.; Golan, D.; Heller, H.; Sharpe, A.; Jilg, N.; Rosenthal, A.; Wong, C. Viral epitope profiling of COVID-19 patients reveals cross-reactivity and correlates of severity. *Science* **2020**, *370* (6520), eabd4250.
(12) Zhang, B.-Z.; Wang, X.; Yuan, S.; Li, W.; Dou, Y.; Poon, V. K.-M.; Chan, C. C.-S.; Cai, J.-P.; Chik, K. K.; Tang, K.; Chan, C. C.-Y.; Hu, Y.-F.; Hu, J.-C.; Badea, S. R.; Gong, H.-R.; Lin, X.; Chu, H.; Li, X.; To, K. K.-W.; Liu, L.; Chen, Z.; Hung, I. F.-N.; Yuen, K. Y.; Chan, J. F.-W.; Huang, J.-D. A novel linker-immunodominant site (LIS) vaccine targeting the SARS-CoV-2 spike protein protects against severe COVID-19 in Syrian hamsters. *Emerg. Microb. Infect.* **2021**, *10*, 874−884.
(13) Lu, Y.; Chan, W.; Ko, B. Y.; VanLang, C. C.; Swartz, J. R. Assessing sequence plasticity of a virus-like nanoparticle by evolution toward a versatile scaffold for vaccines and drug delivery. *Proc. Natl. Acad. Sci. U. S. A.* **2015**, *112*, 12360.
(14) Dalvie, N. C.; Tostanoski, L. H.; Rodriguez-Aponte, S. A.; Kaur, K.; Bajoria, S.; Kumru, O. S.; Martinot, A. J.; Chandrashekar, A.; McMahan, K.; Mercado, N. B.; Yu, J.; Chang, A.; Giffin, V. M.; Nampanya, F.; Patel, S.; Bowman, L.; Naranjo, C. A.; Yun, D.; Flinchbaugh, Z.; Pessaint, L.; Brown, R.; Velasco, J.; Teow, E.; Cook, A.; Andersen, H.; Lewis, M. G.; Camp, D. L.; Silverman, J. M.; Nagar, G. S.; Rao, H. D.; Lothe, R. R.; Chandrasekharan, R.; Rajurkar, M. P.; Shaligram, U. S.; Kleanthous, H.; Joshi, S. B.; Volkin, D. B.; Biswas, S.; Love, J. C.; Barouch, D. H. SARS-CoV-2 receptor binding domain displayed on HBsAg virus-like particles elicits protective immunity in macaques. *Sci. Adv.* **2022**, *8*, No. eabl6015.
(15) Zhang, B.-z.; Hu, Y.-f.; Chen, L.-l.; Yau, T.; Tong, Y.-g.; Hu, J.-c.; Cai, J.-p.; Chan, K.-H.; Dou, Y.; Deng, J.; Wang, X.-l.; Hung, I. F.-N.; To, K. K.-W.; Yuen, K. Y.; Huang, J.-D. Mining of epitopes on spike protein of SARS-CoV-2 from COVID-19 patients. *Cell Res.* **2020**, *30*, 702−704.
(16) Wu, F., R., Yan, M., Liu, Z., Liu, Y., Wang, D., Luan, K., Wu, Z., Song, T., Sun, Y., Ma, Y., Zhang, Q., Wang, X., Li, P., Ji, Y., Li, C., Li, Y., Wu, T., Ying, Y., Wen, S., Jiang, T., Zhu, L., Lu, Y., Zhang, Q., Zhou; J., Huang, Antibody-dependent enhancement (ADE) of SARS-CoV-2 infection in recovered COVID-19 patients: studies based on cellular and structural biology analysis. *medRxiv*, **2020**.
(17) Piccoli, L.; Park, Y.-J.; Tortorici, M. A.; Czudnochowski, N.; Walls, A. C.; Beltramello, M.; Silacci-Fregni, C.; Pinto, D.; Rosen, L. E.; Bowen, J. E.; Acton, O. J.; Jaconi, S.; Guarino, B.; Minola, A.; Zatta, F.; Sprugasci, N.; Bassi, J.; Peter, A.; De Marco, A.; Nix, J. C.; Mele, F.; Jovic, S.; Rodriguez, B. F.; Gupta, S. V.; Jin, F.; Piumatti, G.; Lo Presti, G.; Pellanda, A. F.; Biggiogero, M.; Tarkowski, M.; Pizzuto, M. S.; Cameroni, E.; Havenar-Daughton, C.; Smithey, M.; Hong, D.; Lepori, V.; Albanese, E.; Ceschi, A.; Bernasconi, E.; Elzi, L.; Ferrari, P.; Garzoni, C.; Riva, A.; Snell, G.; Sallusto, F.; Fink, K.; Virgin, H. W.; Lanzavecchia, A.; Corti, D.; Veesler, D. Mapping Neutralizing and Immunodominant Sites on the SARS-CoV-2 Spike Receptor-Binding Domain by Structure-Guided High-Resolution Serology. *Cell* **2020**, *183*, 1024−1042.
(18) Taylor, A.; Foo, S.-S.; Bruzzone, R.; Vu Dinh, L.; King, N. J. C.; Mahalingam, S. Fc receptors in antibody-dependent enhancement of viral infections. *Immunol. Rev.* **2015**, *268*, 340−364.
(19) Katzelnick, L. C.; Gresh, L.; Halloran, M. E.; Mercado, J. C.; Kuan, G.; Gordon, A.; Balmaseda, A.; Harris, E. Antibody-dependent enhancement of severe dengue disease in humans. *Science* **2017**, *358*, 929−932.
(20) Bardina, S. V.; Bunduc, P.; Tripathi, S.; Duehr, J.; Frere, J. J.; Brown, J. A.; Nachbagauer, R.; Foster, G. A.; Krysztof, D.; Tortorella, D.; Stramer, S. L.; García-Sastre, A.; Krammer, F.; Lim, J. K. Enhancement of Zika virus pathogenesis by preexisting antiflavivirus immunity. *Science* **2017**, *356*, 175−180.
(21) Agrawal, A. S.; Tao, X.; Algaissi, A.; Garron, T.; Narayanan, K.; Peng, B.-H.; Couch, R. B.; Tseng, C.-T. K. Immunization with inactivated Middle East Respiratory Syndrome coronavirus vaccine leads to lung immunopathology on challenge with live virus. *Hum. Vaccines Immunother.* **2016**, *12*, 2351−2356.
(22) Vennema, H.; de Groot, R. J.; Harbour, D. A.; Dalderup, M.; Gruffydd-Jones, T.; Horzinek, M. C.; Spaan, W. J. Early death after feline infectious peritonitis virus challenge due to recombinant vaccinia virus immunization. *J. Virol.* **1990**, *64*, 1407−1409.
(23) Shimabukuro, F. H.; Costa, V. M.; Silva, R. C.; Langoni, H.; Silva, A. V.; Carvalho, L. R.; Domingues, P. F. Prozone effects in microscopic agglutination tests for leptospirosis in the sera of mice infected with the pathogenic Leptospira interrogans serovar Canicola. *Mem. Inst. Oswaldo Cruz* **2013**, *108*, 668−670.
(24) Long, Y.; Sun, J.; Song, T.-Z.; Liu, T.; Tang, F.; Zhang, X.; Ding, L.; Miao, Y.; Zhu, W.; Pan, X.; An, Q.; Qin, M.; Tong, X.; Peng, X.; Yu, P.; Zhu, P.; Xu, J.; Zhang, X.; Zhang, Y.; Liu, D.; Chen, B.; Chen, H.; Zhang, L.; Xiao, G.; Zuo, J.; Tang, W.; Zhou, J.; Li, H.; Xu, Z.; Zheng, H.-Y.; Long, X.-Y.; Qin, Q.; Gan, Y.; Ren, J.; Huang, W.; Zheng, Y.-T.; Jin, G.; Gong, L. CoVac501, a self-adjuvanting peptide vaccine conjugated with TLR7 agonists, against SARS-CoV-2 induces protective immunity. *Cell Discov.* **2022**, *8*, 9.
(25) Greaney, A. J.; Starr, T. N.; Barnes, C. O.; Weisblum, Y.; Schmidt, F.; Caskey, M.; Gaebler, C.; Cho, A.; Agudelo, M.; Finkin, S.; Wang, Z.; Poston, D.; Muecksch, F.; Hatziioannou, T.; Bieniasz, P. D.; Robbiani, D. F.; Nussenzweig, M. C.; Bjorkman, P. J.; Bloom, J. D. Mapping mutations to the SARS-CoV-2 RBD that escape binding by different classes of antibodies. *Nat. Commun.* **2021**, *12*, 4196.

https://doi.org/10.1021/acsinfecdis.2c00488
ACS Infect. Dis. XXXX, XXX, XXX−XXX